SSRG International Journal of Mechanical Engineering
ISSN: 2348-8360/ https://doi.org/10.14445/23488360/IJME-V13I7P113

Volume 13 Issue 7, 156-163, July 2026

Original Article

Tribological Performance and Oil Film Strength of MoO_3 Nano-Additized Jatropha Oil Under Boundary Lubrication Conditions

Rushikesh Shirish Pande[1], Bhanudas Dattatraya Bachchhav[2]

[1,2]*Department of Mechanical Engineering, All India Shri Shivaji Memorial Society's College of Engineering, Pune, Maharashtra, India.*

[1]*Corresponding Author : rushikesh.pande89@gmail.com*

Received: 18 April 2026 Revised: 23 June 2026 Accepted: 13 July 2026 Published: 30 July 2026

Abstract *- Due to growing environmental concerns and the depletion of petroleum resources, there is a rising demand for sustainable and biodegradable lubricants. This study examines the tribological performance of Jatropha oil enhanced with molybdenum trioxide (MoO_3) nanoparticles under boundary lubrication conditions. MoO_3 nanoparticles with size ranges of 20–30 nm, 50–60 nm, and 80–90 nm were dispersed into crude Jatropha oil at concentrations of 0.5%, 1.0%, and 1.5% by weight. The lubricants were tested using a four-ball tribotester, and a Taguchi L9 orthogonal array was employed to analyze the influence of nanoparticle size, concentration, load, and speed on wear behavior and oil film strength. The results revealed that additive size is the most influential parameter, followed by load, speed, and concentration. The optimal performance was achieved with 80–90 nm MoO_3 nanoparticles at 1.0 wt.% concentration, 392 N load, and 400 rpm speed. Under these conditions, a significant reduction in wear scar diameter and an increase in oil film strength were observed, attributed to the formation of a stable Mo–O–Fe tribofilm. SEM analysis confirmed smoother worn surfaces and reduced abrasive wear at this composition. The study concludes that MoO_3 nanoparticles significantly enhance the load-bearing capacity, wear resistance, and film strength of Jatropha oil, making it a promising eco-friendly alternative to conventional mineral-based lubricants.*

Keywords *- Jatropha oil, MoO_3, Nano-particles, Oil Film Strength, Wear Scar Diameter.*

1. Introduction

The growing scarcity of petroleum-based lubricants and the environmental hazards associated with their use have led to a shift in focus toward sustainable alternatives. Plant-based oils are gaining more and more interest as environmentally friendly lubricants because of their biodegradability, low cost and good lubrication properties. One of such promising non-edible and bio-derived lubricants is a modified crude Jatropha oil, which can be used in a variety of applications. It was found that transesterified crude Jatropha oil enhances its performance under boundary lubricating conditions. It also showed favorable physicochemical properties to improve lubrication effectiveness for different tribo-pairs [1, 2].

The creation of lubricants with novel nano-additives to enhance the tribological characteristics of vegetable oils is very promising from an environmental point of view. Tribological studies on the effect of different nanoparticles, such as MoS2 [3] and SiO2 [4], metal oxides such as ZnO and TiO2 [5, 6], and carbon nanostructures such as graphene and CNTs [7, 8] have been investigated in large numbers. However, research on Jatropha oil with MoO_3 nanoparticles is still very limited and not explored. Molybdenum trioxide (MoO_3) powder can well reduce the friction coefficient and wear at the sliding interface between aluminum bronze and stainless steel under high temperature conditions [9]. Molybdenum trioxide (MoO_3) is a naturally abundant, inexpensive and environmentally friendly material which has attracted great attention from scientists for different high-impact applications due to its layered structure as well as excellent thermal and chemical stability [10].

The efficiency of lubricant additives in lubricating oils, particularly for hard-coated surfaces, was optimized by investigating the influence of hard coatings on the performance of lubricant additives. Because of the low shear strength offered by the laminar structure of molybdenum based tribofilms, a significant reduction in friction and wear was observed under these conditions [11-13]. Molybdenum trioxide (MoO_3) is a very promising material with great potential for a variety of technological areas, such as large area electrochromic systems, such as displays and smart windows, optical switching films, high-density data storage devices, gas sensors, smart materials and tribological applications as an effective coating material and lubricant additive [14]. Fine particle sizes in the range of 2 to 10 nm with optimal particle morphology and stable crystal structure can be obtained by the synthesis of MoO_3 powder through a combustion reaction. The orthorhombic MoO_3 nanoparticles showed electrochromic properties along with excellent tribo-properties [15, 16].

The strength of an oil film is the ability of a lubricant to maintain a stable protective layer between moving surfaces, reducing friction and wear. It is necessary for the reliable operation of engines, turbines, metalworking processes and industrial equipment. However, in boundary lubrication, this film can be compromised by contact with surface asperities, resulting in higher friction, increased wear and eventual breakdown of the lubricant. Molybdenum-based additives have proved their efficiency to reduce the wear and to maintain the integrity of the contact surfaces in such harsh environments [17, 18].

In [19] tribological properties of Jatropha and Karanja biolubricants were studied for crankshaft bearing applications. A pin-on-disc tribometer with SAE783 aluminum alloy pins against EN31 steel discs was used. [20] . They present the current limitations in synthesizing biolubricants from WCO and the use of natural antioxidants as tunable additives. It discusses and compares different methods for the extraction, physical and chemical modification and characterization of biolubricants derived from WCO. The efficiency of several techniques in the transformation of WCO into biolubricants is evaluated, such as esterification, transesterification and antioxidant inclusion. The paper also discusses the effect of residual bioactive compounds on the oxidative stability and lubricating properties.

Although many studies have been conducted on Jatropha oil with MoS_2 as a nano-additive, research on MoO_3 nano-additives is limited, despite its relatively good oxidation stability. In addition, the effect of MoO_3 nanoparticle size and concentration on wear behavior and oil film strength, which are critical for the development of low-cost lubricants, has not been well studied. The present study deals with the effect of different sizes and concentrations of MoO_3 nanoparticles on the wear characteristics and oil film strength of the bio-lubricants derived from Jatropha.

The aim is to evaluate the overall lubrication efficiency and to find the best additive combination for better tribological performance. Despite extensive research on vegetable oil-based lubricants containing MoS_2, TiO_2, ZnO, graphene, and SiO_2 nanoparticles, limited studies have investigated the tribological behavior of MoO_3 nano-additives in crude Jatropha oil under boundary lubrication conditions. Furthermore, the combined influence of MoO_3 nanoparticle size and concentration on wear scar diameter and oil film strength has not been systematically analyzed using a statistical design of experiments. Therefore, a clear knowledge gap exists regarding the optimization of MoO_3 nano-additized Jatropha oil for sustainable lubrication applications. The novelty of the present work lies in the systematic investigation of MoO_3 nanoparticle size (20-30 nm, 50-60 nm, and 80-90 nm) and concentration (0.5–1.5 wt.%) in crude Jatropha oil using a Taguchi L9 design. The study simultaneously evaluates wear performance and oil film strength while identifying optimum lubrication parameters and correlating tribological behavior with SEM surface morphology.

2. Materials and Methods

2.1. Preparation of Lubricants

The crude Jatropha oil was procured from seeds of the Jatropha curcas L. plant from Super India Enterprises, Udaipur, Rajasthan. The procured MoO_3 nanoparticles size of 20–30 nm, 50–60 nm and 80–90 nm were taken with the weight percent of 0.5%, 1.0%, and 1.5%, respectively to 50 mL batch of crude Jatropha oil, as shown in Figure 1. Each of the mixtures was magnetically stirred for three hours at 800 rpm to obtain a uniform distribution of nanoparticles. Molybdenum trioxide (MoO_3) crystallizes in a layered orthorhombic structure (α-MoO_3 phase), which is composed of distorted MoO_6 octahedra. Here, the six oxygen atoms coordinate to each molybdenum (Mo^{6+}) atom in a distorted octahedron.

The octahedra have edges and corners in common, forming bilayer sheets parallel to the (010) plane. Weak van der Waals forces bind these layers to each other, which results in a lamellar (layered) morphology and anisotropic properties that allow for easy shear and good tribological performance properties, which is why MoO3 has a lamellar (layered) morphology and anisotropic properties. The seeds of Jatropha curcas were collected, and crude Jatropha oil was prepared from the seeds by Super India Enterprises, Udaipur, Rajasthan. The molybdenum trioxide (MoO_3) nanoparticles were purchased from Ultrananotech private limited, Bangalore, with a size range of 20-30 nm, 50-60 nm and 80-90 nm were added to 50 mL batches of crude Jatropha oil in various concentrations, such as 0.5%, 1.0% and 1.5%, as shown in Figure 1.

Each mixture was magnetically stirred for 3 h at 800 rpm to obtain a uniform distribution of the nanoparticles. Molybdenum trioxide (MoO_3) crystallises in a layered orthorhombic structure (α-MoO_3 phase) made up of distorted MoO_6 octahedra. In this type, the coordination of each molybdenum (Mo^{6+}) atom is six oxygens in a distorted octahedron. The bilayers are parallel to the (010) plane, and the octahedra share the edges and corners. The lamellar (layered) morphology of MoO_3 is attributed to the presence of weak van der Waals forces between the layers, which also allows MoO_3 to be easily sheared and have good tribological properties.

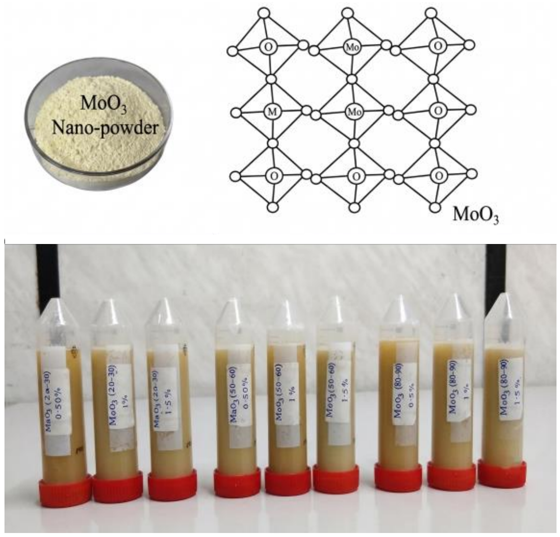

Fig. 1 Nano-powder mixed with different concentration in Jatropha Oil

2.2. Equipment

Jatropha oil was used in the four-ball tribometer (DUCOM TR-30L) to evaluate the performance of MoO_3 nanoparticles. The contact surfaces were chrome steel balls with a diameter of 12.7 mm (AISI E52100 steel, 62–64 HRC). The applied load, spindle speed and lubricant temperature were electronically monitored automatically. All parts in contact with the oil, such as balls, clamping unit and oil cup, were cleaned with a solvent (acetone) prior to each test to avoid contamination. One ball in the setup was clamped in a rotating spindle, and three balls were fixed below in a ball pot such that they were completely immersed in the test oil. The antiwear performance was measured with a tribometer using wear scars of stationary balls. The diameter of the wear scar and the surface area of the scar were measured using a machine vision system after the running process, and the average of the surface area of the scar was used as the data for the lubricant, which was used to investigate the wear resistance. The four-ball tester, ball pot clamping unit, machine vision system and an example wear scar are shown in Figure 2.

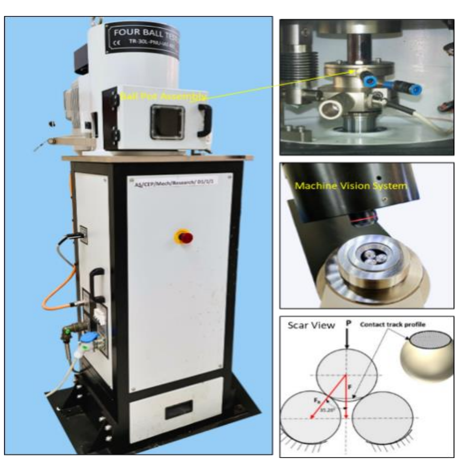

Fig. 2 Four ball tribotester

2.3. Antiwear Performance

The antiwear performance of Jatropha oil containing MoO_3 particles of different sizes was evaluated by conducting tests according to the ASTM D4172-94 standard procedure. A 12.7 mm diameter steel ball was pressed with a 392 N load against the recess made by three tightly held balls into which the pressed ball was placed, and a three-point contact was formed. The test lubricant was kept at a constant temperature of 75 °C. After this temperature was reached, the upper ball was spun for 60 min at 1200 rpm, continuously. After completion of the test, any residual oil on the wear scars was cleaned off using an organic solvent such as acetone and wear scar were measured with the help of a machine vision system. The average diameter of the wear scar for the three fixed balls was then used to characterize the lubricants' ability to reduce wear. Further experiments were conducted to explore the effects of loading and spinning speed by the Taguchi method.

2.4. Evaluation of Oil Film Strength

Developing the film strength of a lubricant is very significant for evaluating its performance in reducing friction and wear in tribological applications, and it will directly affect the life of the components. The film strength is determined as the ratio between the load and the area of the contact forces that occur in the lubricant film. This is usually determined with a 4-ball test arrangement where the upper ball is spinning against three lower balls, as illustrated in Figure 3. Here are three identical steel balls placed in contact with each other in the shape of an equilateral triangle with centers O1, O2, and O3. A fourth ball is located above these balls and touches at points A1, A2 and A3. A vertical load, P, is applied to the top ball (P4) and is distributed evenly between P4P1, P4P2 and P4P3, giving the same reaction force on each of the lower balls (P1 = P2 = P3).

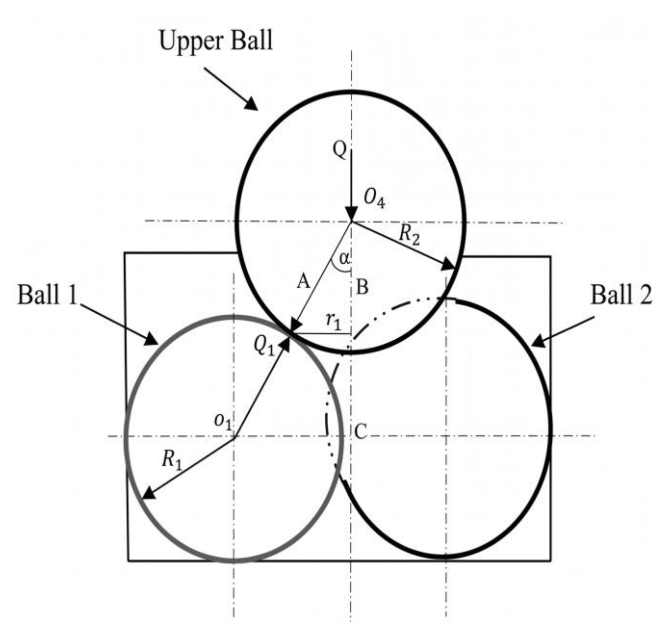

Fig. 3 The sphere calotte for calculating the worn volume on a ball

The three lower balls are tightly fixed onto a rigid fixture, and the upper ball is free to rotate about its vertical axis, while a torque is applied to it. The four-ball tetrahedron configuration is completely immersed in lubricant, providing a simple yet meaningful system for testing the performance of lubricants under simultaneous load and motion in a controlled laboratory environment.

In order to find out the interaction forces between the balls, the directions of the balls, and the angle α (Figure 3) must first be determined. This is done by using geometric analysis, which uses the concept of similar triangles and the following relationship is obtained:

$$\alpha = arcsin\frac{r_1}{R_2} \quad (1)$$

Quantity is defined by the similarity of triangles P4 AB and O4O1C as follows:

$$r_1 = \frac{2R_1R_2}{\sqrt{3}\,(R_1+R_2)} \quad (2)$$

in particular, at R1=R2=R, i.e.,

$$r_1 = \frac{R}{\sqrt{3}} = 0.5774R \quad (3)$$

Hence, angle α is obtained as

$$\alpha = arcsin\frac{2R_1}{\sqrt{3}\,(R_1+R_2)} \quad (4)$$

At R1=R2=R

$$\alpha = \arcsin\frac{1}{\sqrt{3}}$$

Hence,

$$\alpha = 35.26° \quad (5)$$

In order to calculate the normal load (F), the following equation is used

$$F = \frac{P}{3\cos\alpha} \quad (6)$$

Where P is applied Load (N), hence from equations (5) and (6)

$$F = 0.408\ P \quad (6a)$$

Oil film strength (OFS) is calculated as follows [18, 19]

$$\text{Oil Film Thickness} = \frac{F}{A_{ws}} \quad (7)$$

Where A_{ws} is area of wear scar in mm^2.

$$Oil\ Film\ Strenght\ (OFS) = \frac{0.408P}{\frac{\pi d^2}{4}} \quad (8)$$

Where d is average wear scar diameter in mm.

3. Taguchi Design of Experiments

This study focused on the influence of MoO_3 size and concentration, applied loads and operating speeds on wear characteristics, and strength of oil film. Four control variables were studied, with each variable having three levels as shown in Table 1.

Table 1. Parameters and their levels

Parameters	Level 1	Level 2	Level 3
Additive Size (nm)	20-30	50-60	80-90
Additive Concentration (Wt. %)	0.5	1	1.5
Load (N)	392	588	784
Speed (rpm)	400	800	1200

Experiments were designed by Taguchi's L_9 orthogonal array approach. Each test condition was conducted three times to ensure consistency of results, and 27 observations were made to be analyzed. This configuration allowed variance analysis and calculation of signal-to-noise (S/N) ratios.

The output test result is used to compute the S/N ratio, a measure of the consistency of the output that measures the fluctuations in the response. The times for each test was 30 minutes, and the measured responses were converted to the respective S/N ratios. In this study, the "larger-is-better" S/N criterion was used, and in the other study, the "smaller-is-better" S/N was used, as shown in Eqs. (9) and (10) respectively.

$$S/N = -10*\log(\Sigma(1/Y^2)/n) \quad (9)$$

$$S/N = -10*\log(\Sigma(Y^2)/n) \quad (10)$$

Y is the measured data that is observed, and n is the number of times the data was measured.

Various statistical methods, such as Analysis of Variance (ANOVA), were used to derive greater insight and to uncover the most important factors influencing the results.

4. Results and Discussion

4.1. Wear Performance Evaluation

The diameters of the wear scars (WSD) on the three balls below were measured with a machine vision system and software named Scar-view, with a precision of up to 0.001 mm. The average WSD was then calculated and recorded. The results of the experiments are summarized in Table 2. The signal-to-noise (S/N) ratios were computed with the help of MINITAB software.

Table 2. Experimental results (Wear Scar Diameter)

RUN	Additive Size (nm)	Additive Conce. (Wt. %)	Load (N)	Speed (RPM)	WSD 1 (mm)	WSD 2 (mm)	WSD 3 (mm)	Average WSD	SN ratios
1	20-30	0.5	392	400	0.291	0.294	0.284	0.290	10.758
2	20-30	1	588	800	0.342	0.338	0.329	0.336	9.465
3	20-30	1.5	784	1200	0.539	0.524	0.534	0.532	5.477
4	50-60	0.5	588	1200	0.476	0.481	0.486	0.481	6.356
5	50-60	1	784	400	0.345	0.31	0.349	0.335	9.496
6	50-60	1.5	392	800	0.324	0.291	0.312	0.309	10.194
7	80-90	0.5	784	800	0.381	0.358	0.374	0.371	8.610
8	80-90	1	392	1200	0.315	0.304	0.290	0.303	10.367
9	80-90	1.5	588	400	0.308	0.311	0.310	0.310	10.179

The results of the S/N ratio for wear are shown in Table 3, which shows the effects of the applied load (N), the number of rpm, the additive concentration (wt. %), and the particle size of MoO_3 (nm) at three different levels. The delta is the difference between the highest and lowest S/N values and indicates the relative contribution of each factor to the wear behaviour.

Table 3. Response table for Signal-to-Noise Ratio (Wear)

Level	Additive size nm	Additive Concentration (%)	Load (N)	Speed (RPM)
1	8.567	8.575	10.44	10.145
2	8.683	9.777	8.667	9.424
3	9.719	8.617	7.861	7.401
Delta	1.152	1.201	2.579	2.745
Rank	4	3	2	1

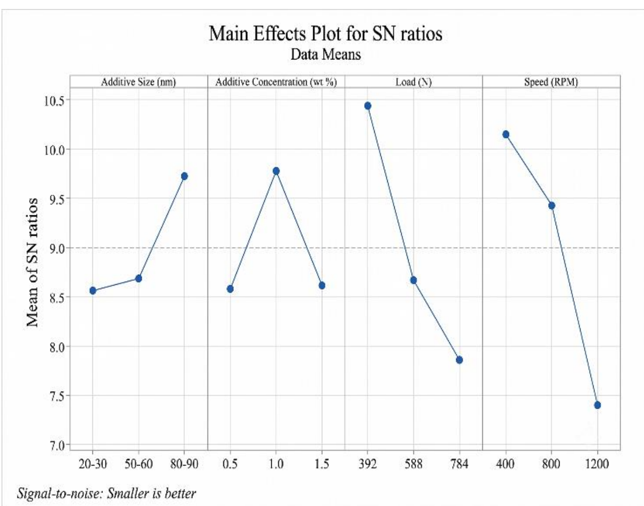

Fig. 4 Main effect plot graph for SN Ratios (Wear)

The effect of the size of the additives, concentration of additives, load, and speed on the performance is shown in Figure 4, with higher SN ratio values denoting better performance according to the “smaller-is-better” criterion. The plot indicates the SN ratio improves as the size of the additive increases up to 80–90, which is the optimum level. The same applies to additive concentration: lower and higher concentrations of the additive are less effective. In the case of load, the SN ratio is best at 392, and reduces considerably with further increase in load, which is beneficial for lower loads.

In terms of speed, the SN is best at 400 and decreases slowly with speed, so it seems that lower speeds provide better performance. Overall, the best set of parameters for better performance is additive size 80-90, additive concentration 1.0, load 392 and speed 400.

The contribution in percentage for each parameter is shown in Table 4. This decrease in SN ratio at a concentration of MoO_3 above 1% is attributed to the loss of effectiveness of the additive at higher concentrations. If the concentration of MoO_3 nanoparticles is below a certain level, the MoO_3 nanoparticles are well dispersed in the lubricant and are able to form a stable tribofilm on the sliding surfaces, effectively reducing wear. But above 1% concentration, the particles will agglomerate, which will not create a uniform film.

These agglomerates can have the effect of abrasive third bodies, which can cause damage rather than protect it. Also, the lubricant may become more viscous, which will impede its flow and reduce the ability to continuously create a lubricating film at the contact surface. Surface saturation is also a factor, as only a certain number of nanoparticles can adhere effectively; the remainder stays suspended and destabilizes the tribofilm. This means that the protection effect decreases and the wear increases with MoO_3 content over 1% concentration.

Table 4. Percentage contribution of parameters

Source	Df	Adj SS	% Contribution
Additive Size (nm)	2	0.017174	09.59
Additive Conce. (Wt %)	2	0.019843	11.08
Load (N)	2	0.058739	32.79
Speed (rpm)	2	0.080986	45.21
Error	0	0.002383	1.33
Total	8	0.179125	100.00

4.2. Assessment of Lubricant Film Strength

The strength of the oil film was estimated based on the dimension of the wear scar calculated by Equation (8). Three stationary balls from the four-ball tester were used for each test, and the scar area on the ball was measured using a machine vision system, which provided accurate and repeatable scar area measurements. These values were then used to calculate the effectiveness of the oil film in holding the surfaces apart under load. The experimental data is detailed with the L9 orthogonal array layout to systematically investigate the effect of various factors and levels. The experimental detail is given based on the L9 orthogonal array to systematically investigate the effect of various factors and levels. Triplicates were run for each test condition to increase the reliability of results. The signal-to-noise (S/N) ratios were investigated using MINITAB software, and the “larger-the-better” method was used to maximize oil film strength. This technique enabled the most important factors influencing the tribological performance of the lubricant to be identified.

Table 5. Experimental results (Oil film strength)

RUN	Additive Size (nm)	Additive Conce. (Wt. %)	Load (N)	Speed (RPM)	OFS1	OFS2	OFS3	Mean OFS	SN Ratios
1	20-30	0.5	392	400	2629	2666	2722	2672	68.53
2	20-30	1	588	800	2423	2352	2264	2346	67.39
3	20-30	1.5	784	1200	1306	1308	1290	1301	62.28
4	50-60	0.5	588	1200	2529	2666	2822	2672	68.51
5	50-60	1	784	400	2050	2221	2423	2231	66.91
6	50-60	1.5	392	800	2806	2965	2908	2893	69.22
7	80-90	0.5	784	800	2908	2965	2867	2913	69.28
8	80-90	1	392	1200	3242	3157	3199	3199	70.09
9	80-90	1.5	588	400	3107	3122	3110	3113	69.86

Table 6. Response Table for Signal to Noise Ratios (examined control factors)

Level	Additive Size (nm)	Additive Conce (Wt. %)	Load (N)	Speed (RPM)
1	66.07	68.78	69.28	68.44
2	68.21	68.14	68.59	68.63
3	69.75	67.12	66.16	66.97
Delta	3.68	1.65	3.12	1.67
Rank	1	4	2	3

Table 6 shows the S/N ratio for the examined control factors. The S/N ratio response analysis can determine the four process parameters' effect. These parameters are the size and concentration of the additive, load, and speed. Additive size is the most impactful, followed by load, speed, and lastly concentration. The concentration of the additive has the smallest impact. This ranking is based on Delta values, which indicate the change of S/N ratios across the levels of the factors.Additive size has the largest positive impact on performance compared to all the other main effects presented in the Figure 5. S/N ratios were clearly greater as the additive size ranged from 20–30 nm to 80–90 nm. In contrast to additive size, the performance effects of other main effects are as follows: S/N ratios decreased as additive concentration increased, increasing load (greater decline observed at 784 N), and greater speed effects (optimal speed set at 800 RPM). To obtain the largest S/N ratios, the 80–90 nm additive size combined with a concentration of 0.5%, a load of 392 N, and a speed of 800 RPM are recommended.

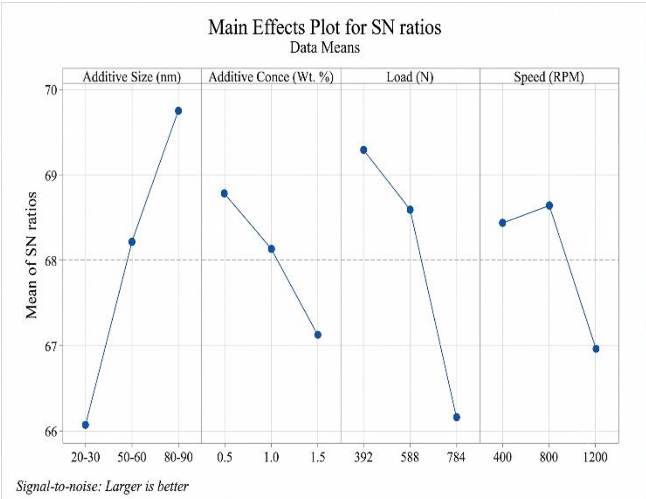

Fig. 5 Main effect plot graph for SN Ratios (OFS)

Table 7 shows the contributions by the four factors of additive size, additive concentration, load, and speed to the variation in the signal-to-noise (S/N) ratio. Additive size is the most significant factor, responsible for 53.31% of the total variation, meanwhile load is responsible for 33.15% of the variation. Additive concentration contributes 7.50%, and speed contributes 6.02%.

The error term has zero degrees of freedom in the presented model, which suggests that the model explains nearly all the variation. It can be concluded that the key factors impacting the system performance are the additive size and load.

Table 7. Analysis of Variance

Source	DF	Adj SS	% Contribution
Additive Size (nm)	2	1442184	53.31
Additive Conce (Wt. %)	2	202924	07.50
Load (N)	2	896683	33.15
Speed (RPM)	2	163086	06.02
Error	0	*	
Total	8	2704878	

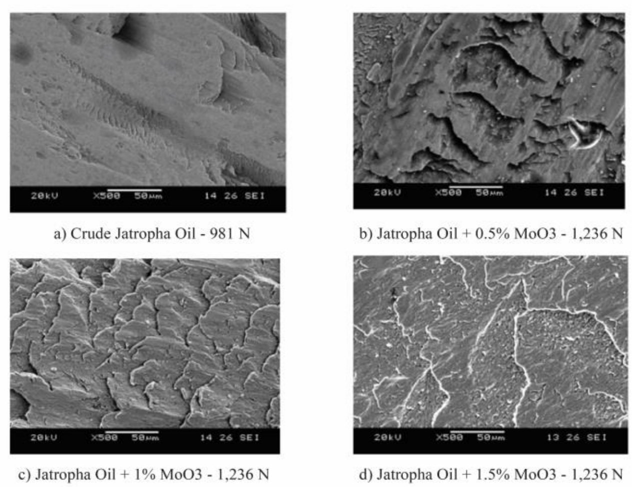

Fig. 6 SEM Micrographs of worn surfaces

4.3. Behavior under Extreme Pressure Conditions

The SEM micrographs (Figure 6) illustrate the worn surfaces of steel lubricated with various mixtures of Jatropha oil subjected to different loads. Image (a) of crude Jatropha oil at 981 N shows distinct, pronounced grooves and extensive ploughing. This is indicative of the lack of protective lubricating film strength and is attributed to the weakening of the lubricating film. Conversely, image (b) shows 0.5 % MoO_3 additive at 1,236 N, where the worn surface is still rough, but more even, illustrating a partial improvement in the reduction of wear that is directly related to an improvement in the degree of the oil's bearing capacity. Image (c) demonstrates that Jatropha oil with 1 % MoO_3 added at the same load exhibits a surface that is overall even and smooth, and that is less so than that of the other images, with extensive grooves, illustrating an effective protective lubricating film that efficiently protects the steel surfaces and reduces wear. On the other hand, image (d) demonstrates the impact of increasing the MoO_3 additive to 1.5 %, where surface crack and delamination of the wear debris from the surface demonstrate that there is a further deterioration of the lubricating properties and is related to an imbalance of the concentration of the bearing additive. Out of the variations of load and oil compositions, the best antiwear performance is observed at the bearing capacity of the MoO_3 additives equaled to 1 % MoO_3, encouraging a balance in the friction protective film. The optimized MoO_3–Jatropha oil formulation demonstrates potential for applications in metal forming, agricultural machinery, hydraulic systems, and other moderate-to-high load tribological systems where biodegradable lubricants are preferred.

5. Conclusion

The addition of MoO_3 nanoparticles significantly improved the tribological performance of crude Jatropha oil. The optimum condition was achieved using 80–90 nm MoO_3 nanoparticles at 1.0 wt.% concentration, 392 N load, and 400 rpm speed. Under these conditions, the lowest wear scar diameter and highest oil film strength were obtained. ANOVA results confirmed that additive size and applied load were the dominant parameters affecting lubricant performance. SEM analysis revealed smoother worn surfaces and evidence of protective tribofilm formation. However, long-term stability, oxidation behavior, and industrial validation remain to be investigated before large-scale implementation.

Limitations and Scope for Future Work

This work focuses on the boundary lubrication condition using a four-ball tribotester and non-processed Jatropha oil as the base lubricant. The long-term stability, Oxide action, and thermal behavior of those nano-lubricants were not studied. The nanoparticle sizes and concentrations were only considered for selected mixtures, and agglomeration/dispersion stability analysis was not done. The assays were performed under laboratory conditions and lacked industrial validation.

The future directions are to assess the lubricant under mixed and hydrodynamic lubrication conditions and in practical applications, including machining and automotive systems. For further improvements in tribological performance, hybrid nano-additives and other biodegradable oils may also be investigated. Therefore, advanced characterization technology like XPS and TEM can be employed to study the formation of tribofilms in detail. More details regarding the rheological, thermal, environmental and economic issues can assist the commercial scale-up of green nano-lubricants.

Conflict of Interest

Author(s) do not have any conflict of interest.

References

[1] N. Talib, and E.A. Rahim, "Performance Evaluation of Chemically Modified Crude Jatropha Oil as a Bio-Based Metalworking Fluid for Machining Process," *Procedia CIRP*, vol. 26, pp. 346-350, 2015. [CrossRef] [Google Scholar] [Publisher Link]

[2] Ganesha Aroor et al., "From Chemistry to Performance: How Nano Additives are Transforming Bio-Lubricants for Enhanced Tribological Applications," *Journal of Molecular Liquids*, vol. 425, pp. 1-18, 2025. [CrossRef] [Google Scholar] [Publisher Link]

[3] Lijie Ma et al., "Investigation of Anti-Friction Properties of MoS_2 and SiO_2 Nanolubricants Based on the Friction Pairs of Inconel 718 Superalloy and YG6 Carbide," *Lubricants*, vol. 13, no. 1, pp. 1-17, 2025. [CrossRef] [Google Scholar] [Publisher Link]

[4] Hong Zhang et al., "Tribological Study of TiO_2 Nanoparticles Modified with Stearic Acid as Additives in Lithium Grease," *Industrial Lubrication and Tribology*, vol. 73, no. 6, pp. 904-910, 2021. [CrossRef] [Google Scholar] [Publisher Link]

[5] Bhanudas Bachchhav, Yash Anecha, and Balraj Waghmare, "Tribological Performance Evaluation of TMPTO based Nano-Lubricants," *Journal of Manufacturing Engineering*, vol. 18, no. 3, pp. 91-95, 2023. [CrossRef] [Google Scholar] [Publisher Link]

[6] Xiaoqiang Fan et al., "Multilayer Graphene as a Lubricating Additive in Bentone Grease," *Tribology Letters*, vol. 55, pp. 455-464, 2014. [CrossRef] [Google Scholar] [Publisher Link]

[7] Yanfei Liu et al., "Graphene-Family Lubricant Additives: Recent Developments and Future Perspectives," *Lubricants*, vol. 10, no. 9, pp. 1-20, 2022. [CrossRef] [Google Scholar] [Publisher Link]

[8] Yoshinori Takeichi et al., "Effects of Molybdenum Trioxide on the Tribological Properties of Aluminum Bronze Under High Temperature Conditions," *Tribology Online*, vol. 4, no. 5, pp. 135-139, 2009. [CrossRef] [Google Scholar] [Publisher Link]

[9] Mário Gomes da Silva Júnior et al., "A Brief Review of MoO_3 and MoO_3-based Materials and Recent Technological Applications in Gas Sensors, Lithium-Ion Batteries, Adsorption, and Photocatalysis," *Materials*, vol. 16, no. 24, pp. 1-26, 2023. [CrossRef] [Google Scholar] [Publisher Link]

[10] Kiichi Nakagome et al., "Friction and Wear Properties of Hard Coatings on Steel Surfaces Under Lubrication with a Fully Formulated Oil with a Mo Additive," *Tribology Online*, vol. 16, no. 1, pp. 59-69, 2021. [CrossRef] [Google Scholar] [Publisher Link]

[11] Y. Rai, A. Neville, and A. Morina, "Transient Processes of MoS_2 Tribofilm Formation under Boundary Lubrication," *Lubrication Science*, vol. 28, no. 7, pp. 449-471, 2016. [CrossRef] [Google Scholar] [Publisher Link]

[12] C. Grossiord et al., "MoS_2 Single Sheet Lubrication by Molybdenum Dithiocarbamate," *Tribology International*, vol. 31, no. 12, pp. 737-743, 1998. [CrossRef] [Google Scholar] [Publisher Link]

[13] R. Yordanov et al., "Characterization of thin MoO_3 Films Formed by RF and DC-Magnetron Reactive Sputtering for Gas Sensor Applications," *Journal of Physics: Conference Series*, vol. 514, pp. 1-6, 2014. [CrossRef] [Google Scholar] [Publisher Link]

[14] G. P. Nagabhushana, D. Samrat, and G. T. Chandrappa, "α-MoO_3 Nanoparticles: Solution Combustion Synthesis, Photocatalytic and Electrochemical Properties," *RSC Advances*, vol. 4, pp. 56784-56790, 2014. [CrossRef] [Google Scholar] [Publisher Link]

[15] Zhu Xiangwe et al., "Preparation of MoO_3 Powder by Hydrothermal Method," *High Temperature Materials and Processes*, vol. 43, no. 1, pp. 1-9, 2024. [CrossRef] [Google Scholar] [Publisher Link]

[16] M.S. Charooa, and M.F. Wania, "Tribological Properties of IF-MoS_2 Nanoparticles as Lubricant Additive on Cylinder Liner and Piston Ring Tribo-Pair," *Tribology in Industry*, vol. 38, no. 2, pp. 156-162, 2016. [Google Scholar] [Publisher Link]

[17] Pramod S. Kathamore, Bhanudas D. Bachchhav, and Manisha B. Bachchhav, "Oil Film Strength Analysis under Boundary Lubrication in TMPTO-based Biolubricant," *Industrial Lubrication and Tribology*, vol. 77, no. 7, pp. 1219-1227, 2025. [CrossRef] [Google Scholar] [Publisher Link]

[18] Amrut S. Aher, and Vijay Kumar Pandey, "Insight on the Effect of Nanoparticles Addition in Oil Lubrication: A Review," *Tribology in Industry*, vol. 45, no. 3, pp. 444-456, 2023. [CrossRef] [Google Scholar] [Publisher Link]

[19] Rajendra V. Pawar, and Dattatray B. Hulwan, "Rheological and Tribological Evaluation of Sustainable Biolubricants Derived from Jatropha and Karanja Oils for Crankshaft Bearing Applications," *Tribology International*, vol. 211, 2025. [CrossRef] [Google Scholar] [Publisher Link]

[20] Jia Leang Teh et al., "Biolubricants from Waste Cooking Oil: A Review of Extraction Technologies, Conversion Techniques, and Performance Enhancement using Natural Antioxidants," *Journal of Environmental Management*, vol. 375, 2025. [CrossRef] [Google Scholar] [Publisher Link]